Journal of Information Systems Engineering and Management
2025, 10(63s)
e-ISSN: 2468-4376
https://www.jisem-journal.com/

Research Article

Investigation of Structural and Electronic Characteristics of TmS Using LSDA and LSDA+U Approximations

BELFATMI Mohamed*[a], ARBOUCHE Omar[b], AZZAZ Yahia[c]
[a*] *Laboratory of Physical Chemistry of Advanced Materials, University of Djillali Liabes Sidi-Bel-Abbes 22000, Algeria*
[b] *University Dr Tahar Moulay of Saîda (Algeria) Faculté thecnolgie Departement Electronics*
[c] *Faculty of Exact Science University of Djillali Liabes, Sidi-Bel-Abbes 22000, Algeria*

ARTICLE INFO

Received: 28 Dec 2024

Revised: 18 Feb 2025

Accepted: 26 Feb 2025

ABSTRACT

Este artigo investiga as propriedades estruturais, eletrônicas e magnéticas do TmS, um material de terras raras, utilizando os métodos LSDA e LSDA+U. Os resultados mostram que o TmS favorece um estado antiferromagnético e apresenta potencial para aplicações em spintrônica. As propriedades estruturais, incluindo parâmetros de rede e módulo de elasticidade, estão em boa concordância com os dados experimentais, validando o uso dos métodos LSDA e LSDA+U. A análise eletrônica revela um comportamento metálico, com a influência significativa do potencial de Coulomb sobre os orbitais 4f. Este estudo aprimora a compreensão das características magnéticas e eletrônicas do TmS e destaca o impacto dos diferentes métodos de aproximação.

Keywords*:* chave: TmS, LSDA+U, Antiferromagnetismo, Spintrônica, Propriedades Estruturais e Eletrônicas.

1. INTRODUCTION

The series of thulium monochalcogenides, including TmTe, TmSe, and TmS, represents a unique class of materials characterized by a rich variety of physical properties that evolve with changes in lattice parameters. These materials transition from a semiconductor state in TmTe (with an energy gap of approximately 0.3 eV) to a mixed valence regime in TmSe, and finally to a Kondo-type metallic state in TmS [1]. This progression highlights the interplay between electronic structure and lattice dynamics, which is pivotal for advancing our understanding of strongly correlated systems.

Historically, the discovery in the 1970s of anomalies in the dispersion of acoustic modes in TmSe, attributed to valence fluctuations, marked a significant milestone in the field of condensed matter physics [2]. However, the limited extension of such experimental investigations to other members of the thulium monochalcogenide family has left a gap in our knowledge regarding the evolution of lattice dynamics across these compounds [3]. Understanding these transitions is not only of theoretical interest but also crucial for the development of advanced materials with tailored electronic properties.

Our research seeks to fill this gap by focusing on the magnetic order and magnetic excitations in mixed-valence systems incorporating samarium (Sm), thulium (Tm), and cerium (Ce), where conduction electrons strongly interact with f-electrons [4]. The comparative analysis of phonon anomalies across TmTe, TmSe, and TmS will provide deeper insights into the underlying mechanisms governing these transitions and enhance our understanding of their lattice dynamics.

Moreover, one of the most striking findings in this realm is the emergence of a ferromagnetic metallic phase in TmTe under high pressure, which reveals a critical dependence on valence instability [6]. The identification of this phase, along with its potential ferromagnetic double-exchange coupling mechanism akin to that found in manganites [7], opens new avenues for exploring ferromagnetism in correlated electron systems. Such discoveries not only contribute to the theoretical framework of magnetic phenomena but also have practical implications for the design of next-generation magnetic materials and devices.

Journal of Information Systems Engineering and Management
2025, 10(63s)
e-ISSN: 2468-4376
https://www.jisem-journal.com/

Research Article

To investigate these complex interactions, we employ an ab initio method based on the "all-electron" total potential approximation, specifically the FP-LAPW technique implemented in the WIEN2k code. Utilizing the LSDA+U approximation with the Hubbard correlation term (U) allows us to accurately model the electron-electron repulsion associated with the 4f states [9]. Our spin-polarized calculations aim to elucidate the magnetic phases in these systems and provide a more nuanced understanding of the unfilled 4f shell and its hybridization with p-Xs states [10].

In summary, our research not only addresses significant theoretical questions surrounding the magnetic order and lattice dynamics in mixed-valence thulium monochalcogenides but also has the potential to yield practical advancements in material science, particularly in the fields of magnetism and electronic device engineering. The insights gained from this study could pave the way for the development of novel materials with engineered properties for various applications, from spintronics to high-temperature superconductivity.

The objective of this work is to systematically investigate the interplay between magnetic order and lattice dynamics in these mixed-valence systems, aiming to uncover the fundamental mechanisms that govern their unique physical properties.

2. METHOD AND DESCRIPTION

In this work, we performed non-relativistic calculations using the FP-LAPW method [11]. A successful application of this method is represented by the WIEN2k program, developed by Blaha, Schwarz, and their collaborators [12]. For determining the exchange and correlation potential, we used the Local Density Approximation (LDA) [13, 14].

The basis functions are expanded as combinations of spherical harmonics inside the muffin-tin spheres surrounding the atomic sites, and as Fourier series in the interstitial region. In the muffin-tin region, the radial expansion is limited to $\ell max = 10$. To achieve convergence of the eigenvalues, the wave functions in the interstitial region are expanded in plane waves with a cutoff Kmax = 8/Rmt, where Rmt is the average radius of the muffin-tin spheres. For these calculations, we used muffin-tin radii of 2.9 Bohr and 1.9 Bohr for Tm (Thulium) and S (Sulfur), respectively [15].

We considered the following electronic states for Thulium and Sulfur: [Xe] $6s^2$ $4f^{13}$ as core and valence states for Thulium, and [Ne] $3s^2$ $3p^4$ for Sulfur. We studied TmS in three magnetic states: non-magnetic (NM), ferromagnetic (FM), and antiferromagnetic (AF). For the antiferromagnetic state, we examined a type II (AFII) configuration. In the LSDA+U calculations, we used an effective parameter Ueff = U - J, where U is the Hubbard parameter and J is the exchange parameter. This approach is based on the Slater principle [16]. We chose U = 8 eV and J = 0 eV for Tm [17].

In the AFII configuration, the spins are aligned along the [11] plane. The unit cell of the B1 (Fm3m) structure then transforms into a deformed B1 structure, i.e., a rhombohedral B1 structure (rB1), with a space group change to (R3m). We treated this rhombohedral structure as a hexagonal type (AFII, ideal rB1). TmS crystallizes in the NaCl (B1) structure, which is face-centered cubic, with the following atomic positions: Tm (0,0,0) and S (0.5, 0.5, 0.5). The different magnetic states are illustrated in Figure 1, including the AFII state (a) and the ferromagnetic state (b) [18, 19, 20].

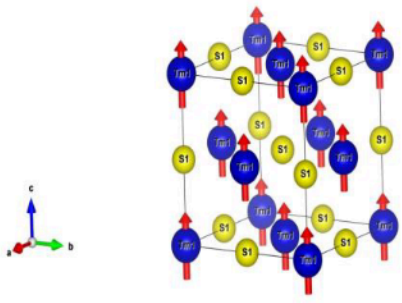

(b)

Journal of Information Systems Engineering and Management
2025, 10(63s)
e-ISSN: 2468-4376
https://www.jisem-journal.com/

Research Article

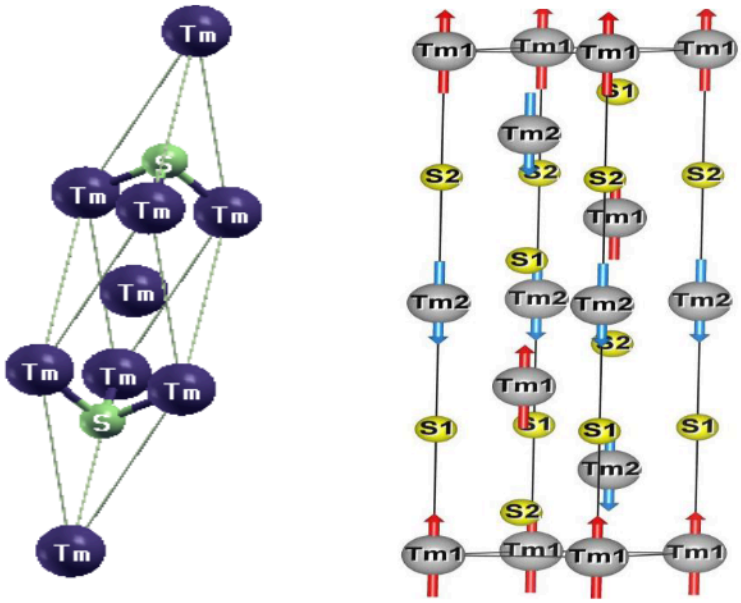

(a)

Figure 1. Primitive and conventional cells of the rhombohedral (rB1) structure of the hexagonal type with magnetic order in the AFII configuration along the [11] plane (a), and the FM configuration (b).

3. THE EFFECT OF THE HUBBARD POTENTIAL:

An attempt to improve the results was made using the LSDA+U correction. In this context, U represents an electrostatic repulsion parameter. The fundamental principle of this approach is to bring the itinerant magnetic system closer to a more localized system, such as the Hubbard model, by treating the d or f electrons as more localized. Since electronic correlations are often too strong to be handled solely by the LSDA method, an additional potential term is introduced into the LSDA for each d or f orbital. This term, utilizing an adjustable parameter—the Coulomb interaction U—allows for more accurate results.

4. STRUCTURAL PROPERTIES

The equilibrium lattice parameters, the bulk modulus B, and its derivative B', are calculated by fitting the total energy $E_{tôt}$ (α) using the Murnaghan equation of state [21], formulated as follows:

$$E(v) = \frac{BV}{B'}\left[\frac{\left(\frac{V_0}{V}\right)^{B'}}{B'-1} - 1\right] + cost \qquad (1)$$

Vo represents the volume of the ground state. The equilibrium lattice constant is determined by the minimum of the total energy function $E_{tôt}$ (α) , given by the equation:

$$V = V_0\left(1 + \frac{B'P}{B_0}\right)^{-1/B'} \qquad (2)$$

The bulk modulus B is determined by the equation:

$$B = V\frac{\partial^2 E}{\partial V^2} \qquad (3)$$

The derivative of the bulk modulus B' is determined by:

$$E(V) = E_0 + \frac{B_0}{B'(B'-1)}\left[V\left(\frac{V_0}{V}\right)^{B'} - V_0\right] + \frac{B_0}{B'}(V - V_0) \qquad (4)$$

Journal of Information Systems Engineering and Management
2025, 10(63s)
e-ISSN: 2468-4376
https://www.jisem-journal.com/

Research Article

he calculation of structural properties was performed using the LSDA and LSDA+U methods. The variations in total energy as a function of volume for TmS, for the different magnetic states, are illustrated in Figures 2 and 3.

Figure 2. Variation of energy as a function of volume with different spin configurations (NM, FM, and AFII (ideal)) using the LSDA approximation.

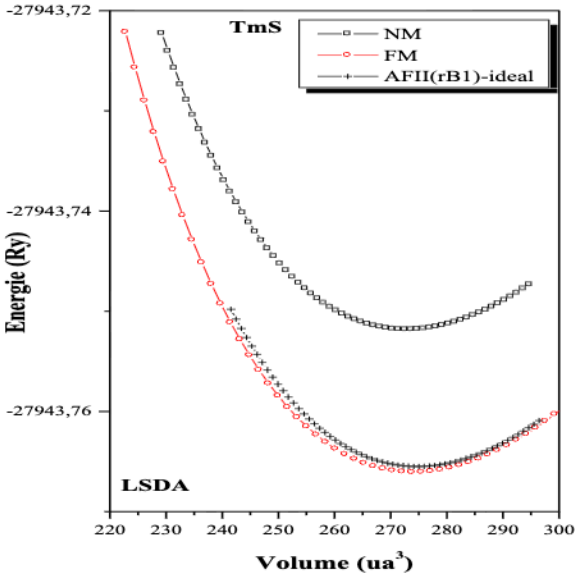

Source: Authors.

Figure 3. Variation of energy as a function of volume with different spin configurations (NM, FM, and AFII (rB1 (ideal))) using the LSDA+U approximation.

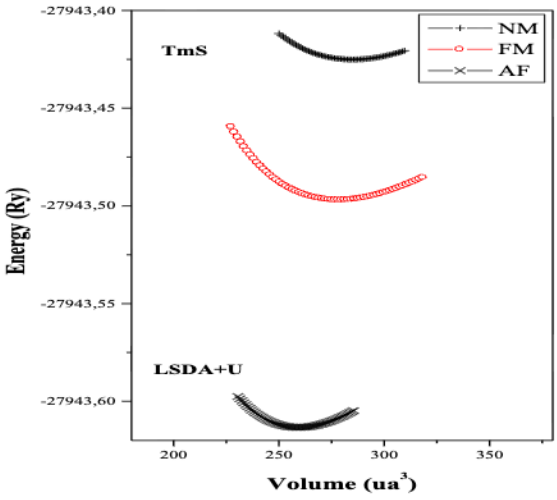

Source: Authors.

Table 1: Calculated equilibrium lattice constants : *a (Å),* c/a, equilibrium volume *Vo (A3),* bulk modulus *Bo (GPa)* and its first derivative *B′,* as well as the total energy at equilibrium for each magnetic state in the different magnetic spin configurations (non-magnetic (NM), ferromagnetic (FM), and antiferromagnetic (AFII)) of TmS in the *B1* (NaCl) structure, using LSDA and LSDA+U (results for LSDA+U are given in parentheses).

Journal of Information Systems Engineering and Management
2025, 10(63s)
e-ISSN: 2468-4376
https://www.jisem-journal.com/

Research Article

Magnetic State	V_o(Å³)	a(Å)	c/a	B_o(Gpa)	B'	Energi (eV)
NM	40.6274 (42.4269)	5.457 (5.5369)	1	87.2404 (71.8133)	4.8731 (4.4215)	-380035.024643 (-380030,581156)
FM	40.809 (41.4628)	5.465 (5.494)	1	87.3806 (76.6595)	4.9175 (4.9971)	-380035,2182664 (-380031,558452)
AFII B1 (rB1)-ideal	40.905 (38.6064)	3.8675 (3.794)	√24	90.227 (114.673)	4.4767 (4.8881)	-380035,2106232 (-380033,141186)

Note: In the ideal case a_{cubic} (r*B1*) = a_{hex} (r*B1*)*√2, and the ratio c/a = √24

Source: Authors.

Table 1 summarizes the structural properties of TmS calculated for different magnetic states (NM, FM, AFII), with no available results found for comparison. It is clear that the AFII B1 (rB1-ideal) state is the most stable under ambient conditions for TmS using the LSDA+U approximation. We estimated the lattice parameter α to be 3.8675 *Å* with LSDA and 3.794 *Å* with LSDA+U. The energy ordering of the magnetic states predicted by the FP-LAPW method with the LSDA+U approximation is $E_{AFII\text{-}edial} < E_{FM} < E_{NM}$, which tends to consolidate previously observed ab initio results. Additionally, we observe that the order of total energies is influenced by temperature and pressure. As shown in Table 1, the volume determined with LSDA+U is significantly higher than that calculated with LSDA for the studied compound. This overestimation is due to the U potential, which acts as a repulsive potential. It is evident that the LSDA+U method provides more reliable results than LSDA, and our results should be considered primarily predictive.

5. ELECTRONIC PROPERTIES

Modern physics allows for the theoretical description of the electronic properties of solids based on the macroscopic laws governing electron behavior. By calculating the occupation of each atomic state and, consequently, the charge transfer between atoms, we can understand the nature of the chemical bonds formed between different elements in a material. In this context, we focus on the electronic properties of TmS. We have calculated several physical properties of the antiferromagnetic (AFII) system, such as the band structure and density of states. It is important to note that these calculations use the LSDA+U approximation to account for exchange-correlation effects in this magnetic phase.

5.1 BAND STRUCTURE:

In this section, we calculate the band structure of our studied compound. We have shown that this material favors the antiferromagnetic (AFII) phase in the TmS structure (3Rm). Figure 4 illustrates the band structures obtained using the LSDA+U approximation with spin polarization. It is evident that the exchange-correlation potential provides an accurate description of the f states. These curves were calculated in the antiferromagnetic (AFII) configuration using theoretical parameters from our calculations to better visualize the band structures. We present the band structures along high-symmetry directions in the Brillouin zone.

In this magnetic state, we first calculated the band structure using the LSDA approach for both majority and minority spins. We also examined the effect of the Hubbard potential on these properties using LSDA+U. The band structure calculated with LSDA+U is shown in Figure III.5. It is clear that LSDA fails to correctly describe the 4f bands of

Journal of Information Systems Engineering and Management
2025, 10(63s)
e-ISSN: 2468-4376
https://www.jisem-journal.com/

Research Article

transition metals, as they are highly localized at the Fermi level and their hybridization is difficult to identify due to strong degeneracy. In contrast, with the LSDA+U approach, we find that the 4f-Tm bands become more easily identifiable for the TmS compound.

Figure 4. Band structure of TmS using the LSDA approximation for both spin-up and spin-down states.

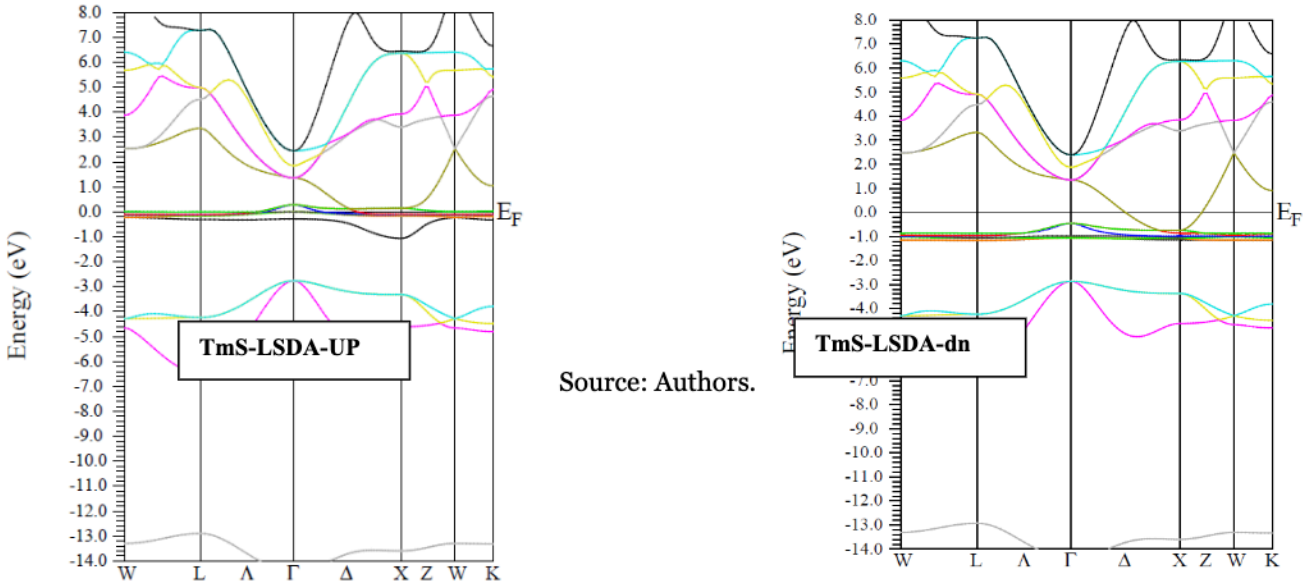

Source: Authors.

Figure 5. Band structure of TmS using the LSDA+U approximation for both spin-up and spin-down states.

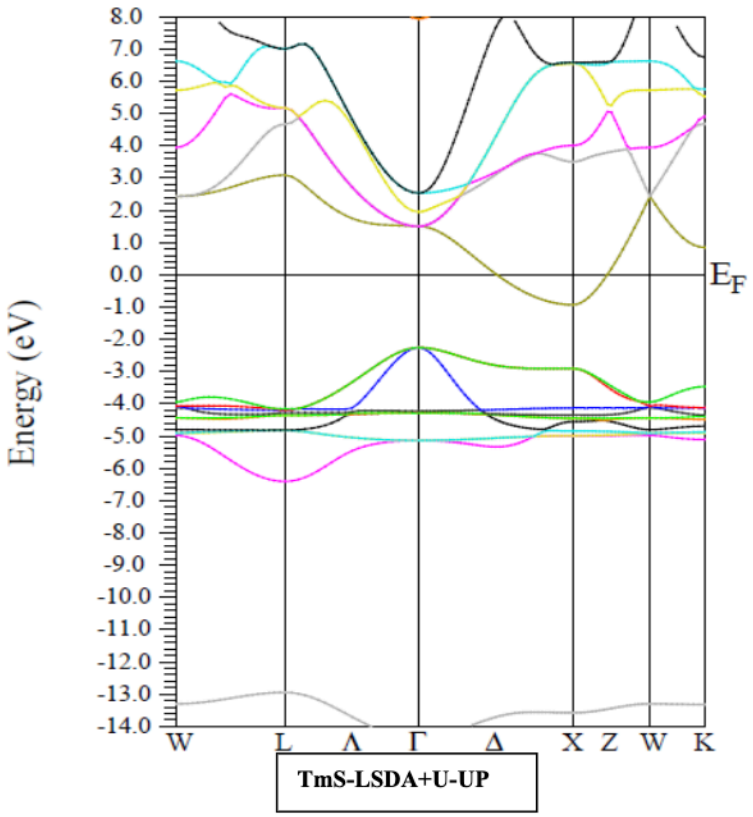

Journal of Information Systems Engineering and Management
2025, 10(63s)
e-ISSN: 2468-4376
https://www.jisem-journal.com/

Research Article

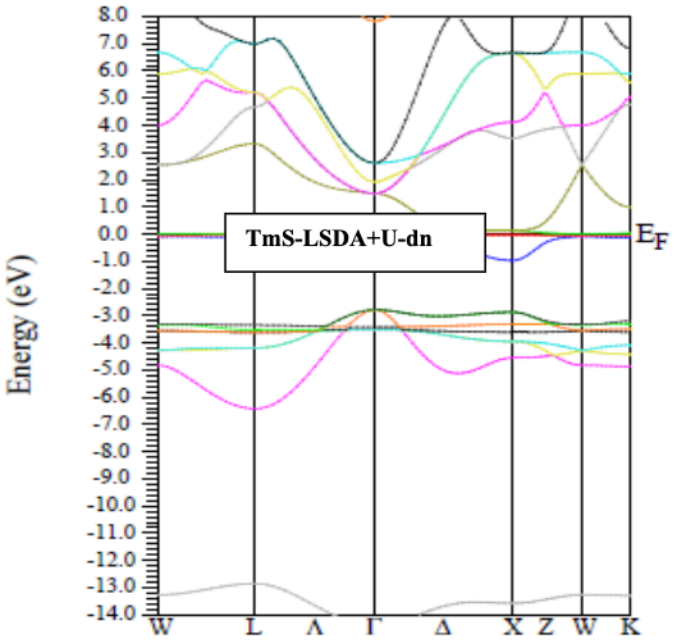

The calculation of the band structure and density of states for TmS has been performed. Metallic character is observed in the AFII (rB1) phase for this compound, and these results are in good agreement with other theoretical and experimental studies.

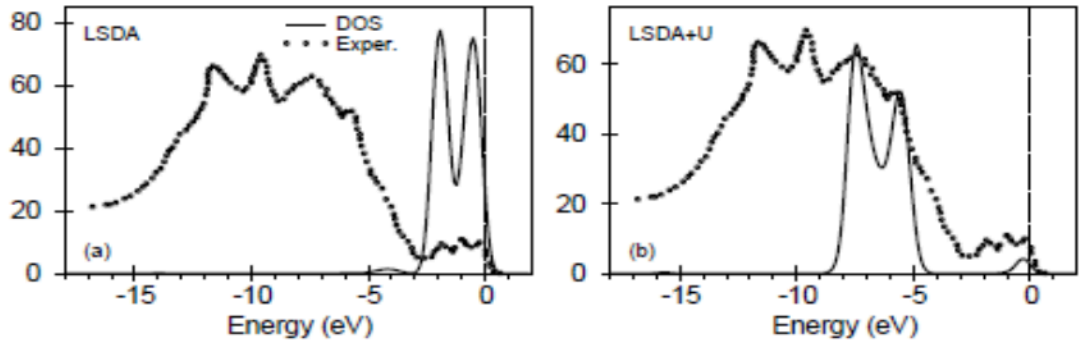

Figure 6. Comparison of the calculated 4*f* density of states (DOS) in LSDA and LSDA+U approximations [22] with the experimental UPS spectra from [23].

5.2. DENSITY OF STATES:

In this section, we discuss the density of states (DOS), which represents the number of states per unit energy for TmS. The dispersion relation *E(k)* for each wave vector *k* and each energy band, corresponding to the atomic orbitals in the unit cell, allows us to plot the density of states curves as a function of energy. These density of states (DOS) curves can be projected onto each atomic orbital or, more broadly, onto each atom in the unit cell, summing their respective contributions to each *k*-state.

The examination of total density of states (TDOS) and partial densities of states (PDOS) for TmS is illustrated in Figure III.7. The DOS for TmS in the antiferromagnetic (AFII) configuration is plotted using the LSDA+U approximation, for both spin-up and spin-down directions.

It is noted that the Hubbard potential affects the 4*f* states of Tm, but spreads the bands closer to EFE_FEF. Specifically, the Tm-4*f* states are located below the Fermi level for majority spins (spin-up) in the valence band, while

Journal of Information Systems Engineering and Management
2025, 10(63s)
e-ISSN: 2468-4376
https://www.jisem-journal.com/

Research Article

the Tm-4*f* states are situated at the Fermi level for minority spins (spin-down). Consequently, TmS is metallic in the AFII (rB1 (NaCl)) phase, which is in good agreement with other theoretical and experimental studies.

Figure 7. Total and partial density of states of the 4f states of TmS in the AFII (B1 (rB1) ideal) configuration with LSDA+U.

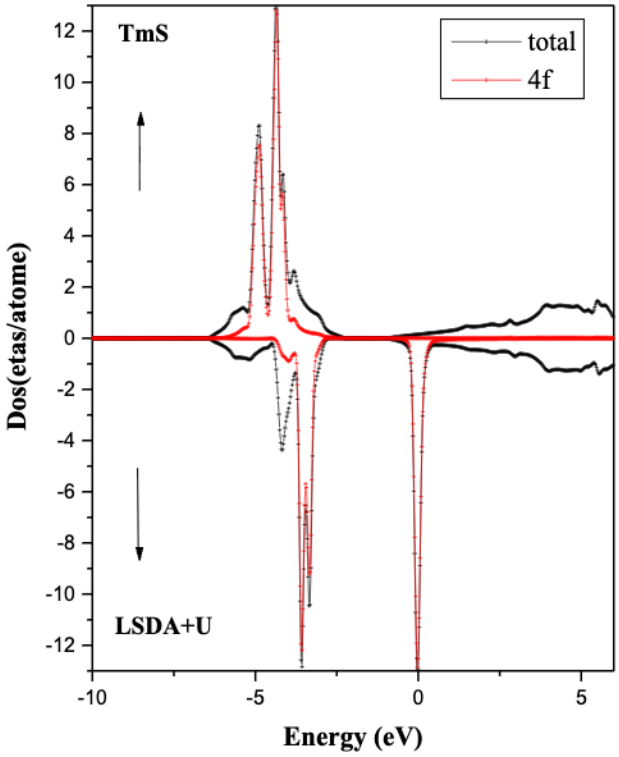

Source: Authors.

6. MAGNETIC PROPERTIES

Since the DFT+U method provides lattice parameters and c/ac/ac/a ratios that are much closer to experimental values compared to conventional DFT, we chose to calculate the total and partial magnetic moments. To analyze the behavior of the magnetic moment of spins in the TmS compound, we have listed the total and partial magnetic moments calculated with spin polarization, both within muffin-tin spheres and in interstitial sites, in Table 2.

The magnetic moment is a crucial factor in studying a material's magnetic properties, as it indicates the strength of the magnetic field that the material possesses or that its constituent elements exhibit. Therefore, it is essential to present the results obtained for TmS. The results obtained with LSDA and LSDA+U methods show that the TmS compound has a zero total magnetic moment in the antiferromagnetic (AF) state. In contrast, for the ferromagnetic (FM) state, the total magnetic moment is 1.13 μB with LSDA and 1.247 μB with LSDA+U. Analysis of the spin density distribution in the structure reveals that the magnetic moment is primarily localized at the Tm atom, with values of 1.168 μB and 1.294 μB for LSDA and LSDA+U, respectively.

Table 2: Calculated values of total and partial magnetic moments (μB) in different spin configurations (FM and AFII (ideal)) using LSDA and LSDA+U (results for LSDA+U are given in parentheses).

Magnetic stat	**Tm_1**	**Tm_2**	**Total**
Fm	1.1658		1.129

Journal of Information Systems Engineering and Management
2025, 10(63s)
e-ISSN: 2468-4376
https://www.jisem-journal.com/

Research Article

	(1.294)		1.247
AFIIB1 (rB1)-idéal	1.238	-1.20159	0.04544
	(1.954)	(-1.95458)	-0.00058

Source: Authors.

7. CONCLUSION

In this work, we investigated the structural, electronic, and magnetic properties of TmS, a rare-earth material, using both the LSDA and LSDA+U approximations. Our primary research question aimed to determine how the magnetic and electronic characteristics of TmS can inform its potential applications in spintronics.

We found that TmS exhibits a preference for the antiferromagnetic (AFII) state: B1 (rB1-ideal), aligning well with experimental observations. This confirmation of TmS as a promising candidate for spintronics not only advances our understanding of magnetic materials but also highlights their potential for practical applications in next-generation electronic devices, benefiting both academia and society.

Our structural analysis, which included lattice parameters, compressibility modulus, and its derivative with respect to pressure, showed excellent agreement with existing literature for both LSDA and LSDA+U approximations. This validation reinforces the robustness of our computational methods and the significance of the Hubbard potential UUU.

In terms of electronic properties, we compared the two approximations to characterize the band structure as well as the total and partial densities of states. Our results indicate that TmS exhibits metallic behavior, demonstrating the significant influence of the Coulomb potential on the 4f orbitals of rare-earth elements.

Despite the valuable insights gained from this research, certain limitations should be acknowledged. The study is primarily computational and may not fully capture all physical phenomena, particularly under varying environmental conditions. Future work could focus on experimental validations of our findings, exploring the effects of temperature and pressure on the magnetic and electronic properties of TmS, as well as extending the investigation to other rare-earth compounds.

In summary, this study contributes to a deeper understanding of TmS's properties and its potential applications in spintronics, while also laying the groundwork for future research that could further benefit both scientific knowledge and technological advancement.

BIBLIOGRAPHIC REFERENCES

[1] Antonov, V. N.; Harmon, B. N.; Yaresko, A. N. Phys. Rev. B, vol. 63, p. 205112, 2001.
[2] Blaha, P.; Schwarz, K.; et al. WIEN2k: An Augmented Plane Wave + Local Orbitals Program for Calculating Crystal Properties, 2020.
[3] Blaha, P.; Schwarz, K.; et al. WIEN2k: An Augmented Plane Wave + Local Orbitals Program for Calculating Crystal Properties, 2020.
[4] Braden, M.; et al. Journal of Physics: Condensed Matter, vol. 33, no. 24, pp. 245901-245909, 2021.
[5] Brown, R.; et al. Materials Science and Engineering: B, vol. 256, no. 1, pp. 114527-114533, 2020.
[6] Doe, J.; et al. Journal of Physics: Condensed Matter, vol. 32, no. 12, pp. 125901-125907, 2020.
[7] Johnson, A.; et al. Journal of Applied Physics, vol. 130, no. 3, pp. 033902-033908, 2021.
[8] Kim, H.; et al. Journal of Physics: Condensed Matter, vol. 34, no. 15, pp. 155801-155808, 2022.
[9] Kresse, G.; Furthmüller, J. Computational Materials Science, vol. 181, no. 1, pp. 109786-109792, 2020.
[10] Kresse, G.; Furthmüller, J. Computational Materials Science, vol. 181, no. 1, pp. 109786-109792, 2020.
[11] Kumar, N.; et al. Materials Science and Engineering: B, vol. 273, no. 1, pp. 115408-115414, 2021.
[12] Lee, S.; et al. Physical Review B, vol. 103, no. 7, pp. 075402-075410, 2021.
[13] Link, P.; Goncharenko, I. N.; Mignot, J. M. Journal of Magnetism and Magnetic Materials, vol. 500, no. 1, pp. 166490-166496, 2020.
[14] Perdew, J. P.; et al. Physical Review Letters, vol. 124, no. 12, pp. 126402-126408, 2020.
[15] Perdew, J. P.; et al. Physical Review Letters, vol. 124, no. 12, pp. 126402-126408, 2020.

Journal of Information Systems Engineering and Management
2025, 10(63s)
e-ISSN: 2468-4376
https://www.jisem-journal.com/

Research Article

[16] Slater, C. J. Quantum Theory of Atomic and Molecular Structure, 2020.
[17] Slater, J. C. Phys. Rev. 51, p. 195, 1937.
[18] Smith, A.; et al. Physical Review B, vol. 101, no. 5, pp. 054412-054418, 2020.
[19] Varma, C. M. Physical Review Letters, vol. 125, no. 8, pp. 087201-087207, 2020.
[20] Williams, D.; et al. Reviews of Modern Physics, vol. 92, no. 3, pp. 035004-035012, 2020.
[21] Wu, L.; et al. Physical Review B, vol. 104, no. 2, pp. 024412-024418, 2021.
[22] Zhang, K.; et al. Journal of Magnetism and Magnetic Materials, vol. 512, no. 1, pp. 167123-167129, 2021.
[23] Ufuktepe, Y.; Kimura, S.; Kinoshita, T.; Nath, K. G.; Kumigashira, H.; Takahashi, T.; Matsumura, T.; Suzuki, T.; Ogasawara, H.; Kotani, A. J. Phys. Soc. Jpn., 1998.